Available online at www.sciencedirect.com

ScienceDirect

Ceramics International 40 (2014) 1229–1234

CERAMICS INTERNATIONAL

www.elsevier.com/locate/ceramint

Short communication

One-pot synthesis of NaA and NaP zeolite powders using agro-waste material and other low cost organic-free precursors

Subha Bohra, Debtosh Kundu, Milan Kanti Naskar*

Sol–Gel Division, CSIR-Central Glass and Ceramic Research Institute, Kolkata 700032, India

Received 20 March 2013; received in revised form 18 April 2013; accepted 1 June 2013
Available online 25 June 2013

Abstract

NaA and NaP zeolite powders were synthesized by hydrothermal condition at 100 °C/15–96 h using agro-waste material, rice husk ash as silica source in the presence of other organic-free low cost precursors like aluminum foil, sodium hydroxide and water. The powders were characterized by thermogravimetric analysis (TGA), differential thermal analysis (DTA), powder X-ray diffraction (PXRD), Fourier transform infrared (FTIR) spectroscopy, N_2 physisorption studies, and field emission scanning electron microscopy (FESEM). The BET surface area values of NaA and NaP powders were in the range of 348–179 $m^2\ g^{-1}$ and 129–85 $m^2\ g^{-1}$, respectively. FESEM images showed flower-like morphology for the NaA powders obtained at 100 °C/15 h, and broken cashew-nut-like morphology for the NaP powders synthesized at 100 °C/72 h.

Keywords: B. Porosity; Microstructure; Rice husk ash; NaA and NaP zeolites

1. Introduction

Zeolites are hydrated crystalline microporous aluminosilicates composed of tetrahedral TO_4 units (T = Si or Al) which are linked together by sharing of oxygen atoms to form regular intracrystalline cavities and channels of atomic dimensions. Because of molecular sieve properties along with high thermal, mechanical and chemical stabilities, zeolites are extensively used as catalysts, adsorbents, ion exchangers, liquid and gas separation, and membranes [1,2].

The NaA zeolite has a cubic structure of three dimensional pore system having pore opening of 0.42 nm. The unit-cell formula of NaA zeolite is $Na_{12}[(AlO_2)_{12}(SiO_2)_{12}].27H_2O$. The NaP zeolite has gismondine (GIS) framework topology with two dimensional channels in elliptical pore openings of 0.31 nm × 0.44 nm and 0.26 nm × 0.49 nm. The unit-cell formula of NaP zeolite is $Na_6[(AlO_2)_6(SiO_2)_{10}].15H_2O$. Because of their smaller pore dimensions, both the NaA and NaP zeolites are useful for the separation of small gas or liquid molecules, particularly for the removal of toxic and radioactive waste species from waste water. These zeolites also find application for the formation of environmentally friendly detergents [3].

Synthesis of NaA and NaP zeolites from low cost precursors becomes important for their industrial production. Rice husk is an abundantly available agriculture waste materials containing maximum amount of siliceous ash. Burning of rice husk in air produces rice husk ash (RHA) containing 85% to 98% silica. The burned rice husk causes environment pollution [4]; the combustion of rice husk produces green house gas, CO_2 which is responsible for global warming. RHA may cause eye sore, respiratory diseases such as asthma, bronchitis, malfunction of lungs etc. The presence of crystalline silica e.g. quartz and cristobalite in RHA at high temperature [5] may cause health hazard like silicosis. Therefore, useful applications of rice husk are desirable to mitigate environment pollution and health hazard. We have reported the utilization of RHA for the synthesis of zeolites like hydroxy sodalite [6], ZSM-11 [7], and ZSM-5 [8,9]. Synthesis of NaA zeolite from rice husk ash has been reported by many authors [10–13].

In the reported literature, for the preparation of zeolites from RHA, the silica is first extracted separately as silicate from RHA followed by the synthesis of zeolites with the extracted

---

*Corresponding author. Tel.: +91 33 2473 3496x3516; fax: +91 33 24730957.
E-mail address: milan@cgcri.res.in (M.K. Naskar).

0272-8842/$ - see front matter © 2013 Elsevier Ltd and Techna Group S.r.l. All rights reserved.
http://dx.doi.org/10.1016/j.ceramint.2013.06.001

silicate. The process is time consuming and tedious. In the present investigation, we report a facile one-pot hydrothermal synthesis of NaA and NaP zeolite powders through in-situ extraction (extraction and conversion of desire product in single-step process) of silica as silicate from RHA. In this method, the intermediate reaction steps for the extraction of silica from RHA could be omitted following a simple process. In this work, the effect of synthesis time on the crystallization, microstructural and textural properties of the prepared NaA and NaP powders was studied. As the present method of preparation of zeolites starts with the agriculture waste material, RHA and other aqua-based precursor materials, it will be advantageous as a low cost process and beneficial for controlling environment pollution as well.

2. Experimental

2.1. Material and synthesis of zeolite NaA and NaP powders

Rice husk ash was obtained by calcination of partially burned ash (collected from local rice mill) at 700 °C for 6 h with heating and cooling rates of 4 °C/min each in air atmosphere. Sodium hydroxide (G.R., Merck, India, purity $>98\%$), aluminum metal foil (A.R. S.D. Fine-Chem Ltd., India) and deionized water were used as other starting materials.

Fig. 1 shows a schematic representation for the preparation of NaA and NaP zeolites. Sodium aluminate solution was prepared by dissolving aluminum metal foil with required quantity of NaOH solution in water. A particulate suspension was made by mixing RHA and sodium aluminate solution with a molar composition of $2.1Na_2O{:}Al_2O_3{:}3.8SiO_2{:}50H_2O$. It was then stirred for 15 h to obtain a dispersion. The dispersion prepared as above was transferred into Teflon-lined stainless steel autoclaves, and heated separately at 100 °C for 15 h, 24 h, 48 h, 72 h and 96 h under autogeneous pressure to obtain NaA and NaP zeolite powders. After hydrothermal reaction, the as-prepared powders were collected by centrifugation (9000 rpm) followed by washing with water repeatedly until the washing liquid became almost neutral (pH ~7). The washed powders were dried at 80 °C for 4 h.

2.2. Material characterization

The chemical composition of RHA was determined by X-ray fluorescence (XRF) analysis (PANalytical, Model: Axios, Almelo, the Netherlands). The particle size of RHA was analyzed by Microtrac (Model: S3500, USA) laser diffraction particle size analyzer. The thermal behaviors of the as-prepared zeolite powders were studied by differential thermal analysis (DTA) and thermogravimetric analysis (TGA) (Netzsch STA 449C, Germany) from 30° to 800 °C at the heating rate of 10 °C/min in air atmosphere. The powder X-ray diffraction (PXRD) study of the sample was carried out by a Philips X'Pert Pro XRD (Model: PW 3050/60) with Ni-filtered Cu-K_α radiation ($\lambda = 0.15418$ nm), operating at 40 kV and 30 mA. The characteristic vibration bands of the powders were confirmed by Fourier transform infrared (FTIR) spectroscopy (Nicolet 5PC, Nicolet Analytical Instruments, Madison, WI) using the KBr pellet method with the resolution of 4 cm^{-1} and scan of 100. Nitrogen adsorption and desorption studies were performed at liquid nitrogen temperature (77 K) with a Quantachrome (ASIQ MP) instrument. The morphology of RHA and synthesized powders was studied by FESEM (Model: Zeiss, Supra™ 35VP, Oberkochen, Germany) operating with an accelerating voltage of 10 kV.

3. Results and discussion

The XRF analysis of RHA showed the compositions (wt%) of SiO_2 (95.54%), Al_2O_3 (0.78%), K_2O (0.72%), P_2O_5 (1.45%), MgO (0.60%), CaO (0.29%), Fe_2O_3 (0.23%), Na_2O (0.10%), MnO (0.05%), TiO_2 (0.02%) and SO_3 (0.22%). Fig. 2 shows (a) XRD, (b) particle size distribution, and (c) FESEM image of RHA. The XRD peak of RHA exhibited a broad hump at the 2θ of around 20°–22° which indicated the amorphous nature of RHA. However, a minor crystallization of α-quartz phase ($2\theta = 26.7°$) (Fig. 2a) was also noticed in RHA. It is reported that during calcination, the removal of organic matter of rice husk could lead to the crystallization of amorphous silica in rice husk [14] and it became more pronounced for uncontrolled calcination [15]. A wide particle size distribution (Fig. 2b) with d_{50} of 28.5 μm was observed

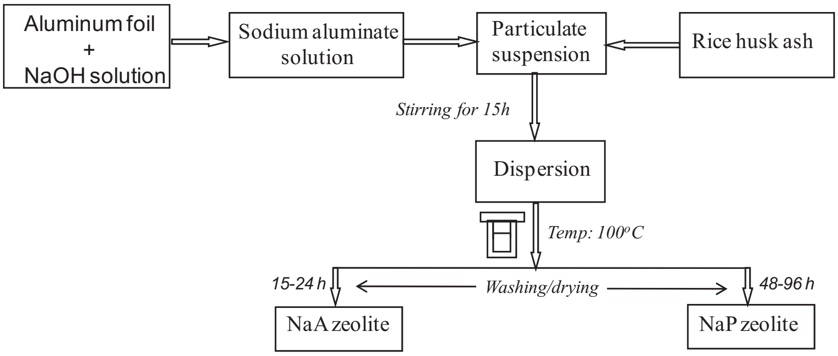

Fig. 1. Schematic representation for the preparation of NaA and NaP zeolite powders.

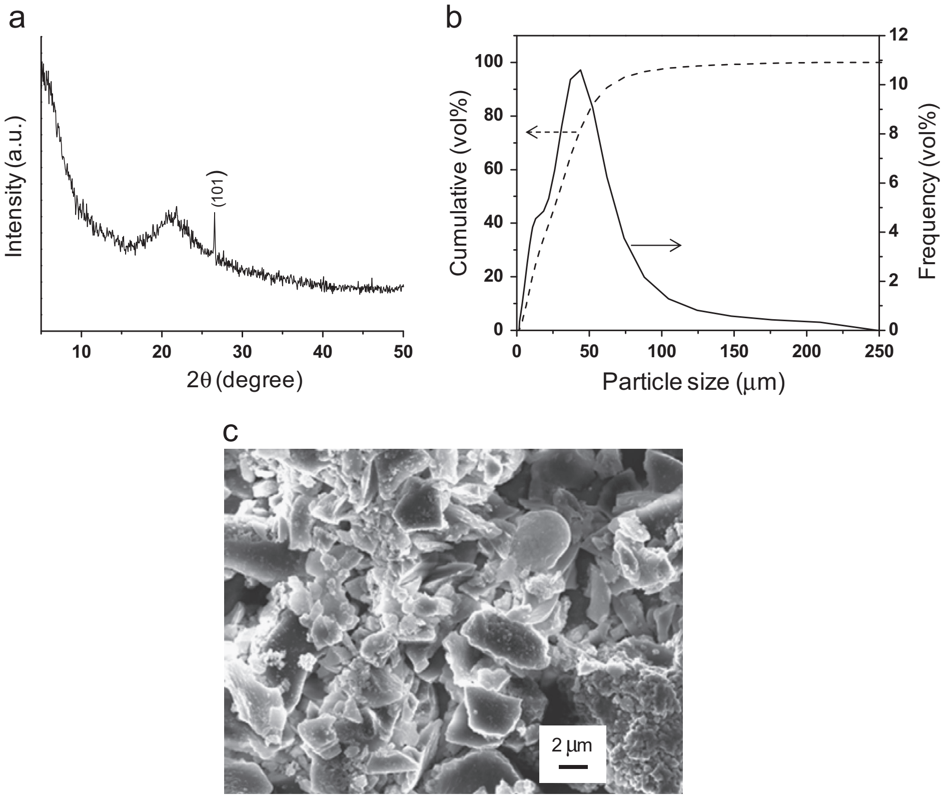

Fig. 2. (a) XRD, (b) particle size distribution, and (c) FESEM image of RHA calcined at 700 °C/6 h.

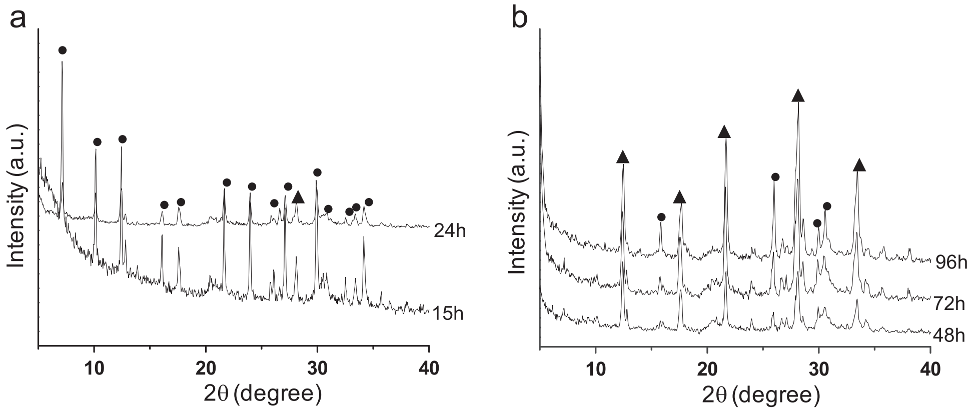

Fig. 3. XRD patterns of (a) NaA and (b) NaP zeolite powders ●: NaA; ▲: NaP."

for RHA. It indicated that RHA particles had different size ranges. It was also supported by the FESEM image (Fig. 2c) of RHA which revealed irregular shape of the particles having different sizes.

Fig. 3 shows the XRD patterns of (a) NaA (JCPDS no. 39-222) and (b) NaP (JCPDS no. 71-0962) zeolites obtained at 100 °C for 15–24 h and 48–96 h, respectively. It is interesting to point out that a trace amount of NaP phase was obtained in the presence of NaA phase for the reaction time of 15–24 h at 100 °C (Fig. 3a). On the other hand for 48–96 h of reaction time at 100 °C, minor crystalline phase of NaA was observed along with NaP phase (Fig. 3b). The formation of NaA and NaP crystals obtained at 100 °C for different time periods was also supported by FTIR studies (Fig. 4). Fig. 4a shows the characteristics absorption bands of NaA zeolite [16]. The absorption band at 550 cm^{-1} was due to the D4R of NaA, and the other bands appeared at 465 cm^{-1}, 673 cm^{-1} and 1001 cm^{-1} corresponded to Si–O–Al bending, Si–O–Al symmetric stretching, and Si–O–Al asymmetric stretching vibrations, respectively of the same powder. The FTIR spectra of NaP zeolite [17] is shown in Fig. 4b. The bending vibration of TO_4 (T = Si, Al) of NaP was recorded at around 430–512 cm^{-1}. The symmetric stretching vibrations of Si–O and Al–O were noticed at 610 cm^{-1}, 697 cm^{-1} and 745 cm^{-1}

while the asymmetric stretching vibration was observed at 1014 cm^{-1}.

Fig. 5 shows the DTA and TG curves of (a) NaA and (b) NaP powders. In DTA curves, a broad endothermic peak was found at 150 °C for NaA powder while NaP powder showed the endothermic peak at 135 °C. It indicated the removal of adsorbed water from the gel powders. The TG curve of NaA powder showed a mass loss of about 18% and that of NaP powder revealed the mass loss of 16% up to 350 °C for each sample. Therefore, no significant changes in mass losses for NaA and NaP powders were noticed. Fig. 6 shows the N_2 adsorption and desorption isotherms of (a) NaA and (b) NaP zeolites synthesized at 100 °C for different time periods. It indicated that the initial steep micropore uptake took place at about $p/po < 0.02$. The uptake of nitrogen increased steeply above the relative pressure of about 0.8. The curves show an IUPAC type IV isotherm in which the hysteresis loops were due to the formation of textural mesoporosity originated from the intergrowth of the crystals. The mesopores generated during the formation of zeolite crystals (NaA and NaP) were slit-like shaped [8]. The textural properties (BET surface area, total pore volume, and average pore size) of the samples synthesized at 100 °C for different time periods are shown in Table 1. It was noticed that for NaA zeolite, the BET surface area, and total pore volume decreased with increase in synthesis time from 15 h to 24 h; however, there was no significant change in average pore sizes. The NaA zeolite obtained at 100 °C/15 h showed the maximum BET surface area of 348 $m^2\ g^{-1}$. Some amorphous particles coexisting with NaA zeolite obtained at 100 °C/15 h could contribute for high BET surface area. For NaP zeolite, the BET surface area and total pore volume also decreased with the increasing reaction times from 48 h to 96 h. A minimum pore volume and smallest average pore size for 100 °C/96 h-treated NaP sample was due to the more abundance of micropores in NaP zeolite.

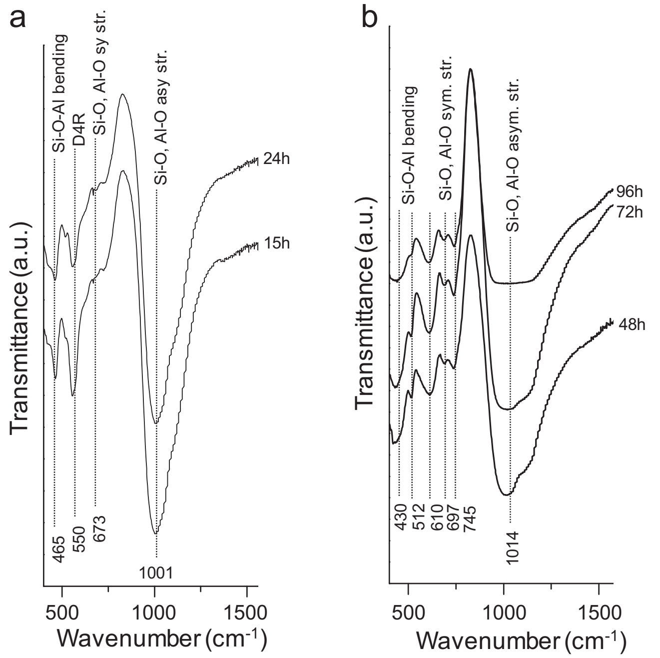

Fig. 4. FTIR spectra of (a) NaA and (b) NaP zeolite powders.

Fig. 7 shows the FESEM microstructures of NaA zeolite powders obtained at 100 °C for (a) 15 h, (b) 24 h, and those of NaP zeolite powders synthesized at 100 °C for (c) 72 h and (d) 96 h. It was observed that for 15 h of reaction time, flower-like morphology for the NaA zeolite was obtained. After the reaction time of 24 h, cube-shaped NaA particles were obtained. However, for the NaP zeolite, a broken cashew-nut-like morphology was obtained at 100 °C for 72 h. With further increase in synthesis time up to 96 °C, the particles got fragmented forming nanometer-size NaP powders. Therefore, with the same molar composition of the precursors at a fixed temperature (100 °C), by changing the reaction times from 15 h to 96 h, two different types of zeolites, NaA and NaP were formed with varying morphologies. It is mentioned worthy that initially (15 h of reaction time) flower-like NaA zeolite was formed surrounding small rice husk particles which could act as nucleating sites for particle growth. Some amorphous particles could coexist with the flower-like particles of NaA, which was evident from higher BET surface area and pore volumes. With increase in reaction time up to 24 h, well-crystalline cube-shaped NaA particles were formed. With further increase in reaction time (48–96 h), metastable NaA zeolite was transformed to more thermodynamically stable NaP

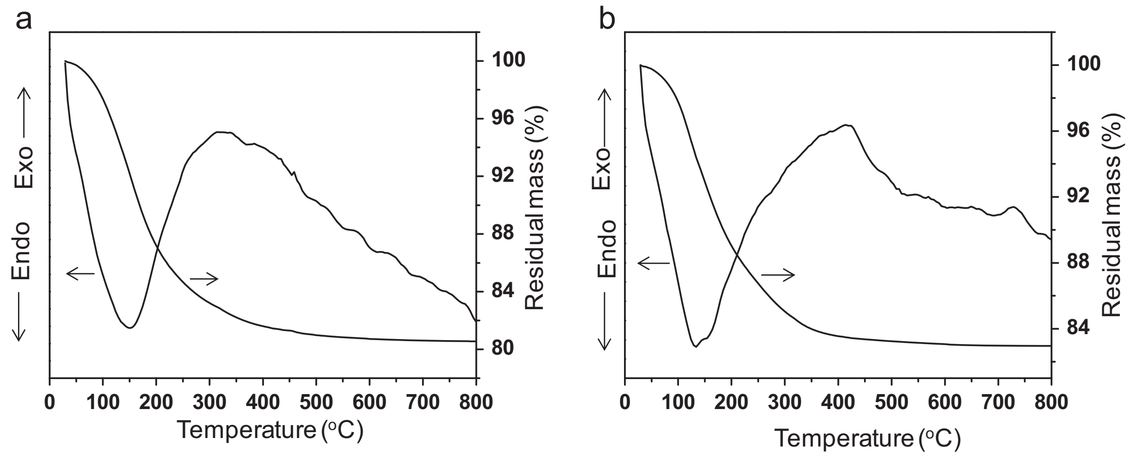

Fig. 5. DTA and TG curves of (a) NaA and (b) NaP zeolite powders.

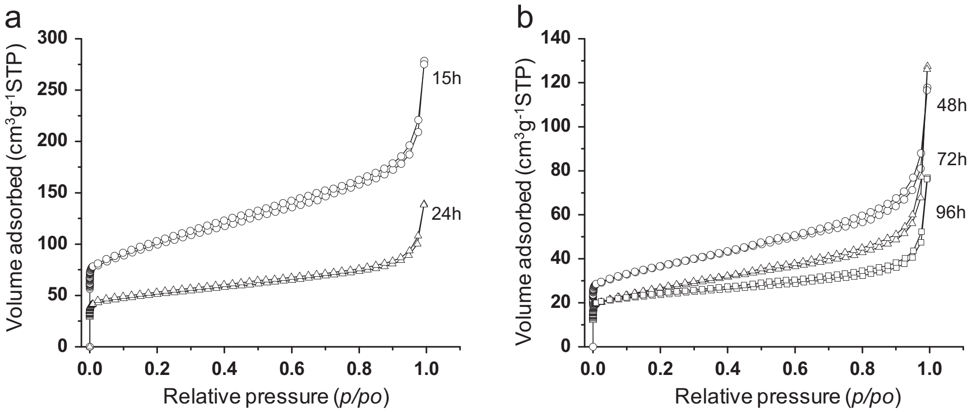

Fig. 6. Nitrogen adsorption and desorption isotherms of (a) NaA and (b) NaP zeolite powders.

Table 1
The textural properties of NaA and NaP zeolite powders synthesized at 100 °C.

Synthesis time (h)	Zeolite	S_{BET} (m^2 g^{-1})[a]	$V_{\mathrm{p-total}}$ (cm^3 g^{-1})[b]	d_{p} (nm)[c]
15	NaA	348	0.43	4.9
24	NaA	179	0.21	4.8
48	NaP	129	0.19	5.6
72	NaP	92	0.18	8.6
96	NaP	85	0.12	2.8

[a] BET surface area.
[b] Total pore volume.
[c] Average pore size.

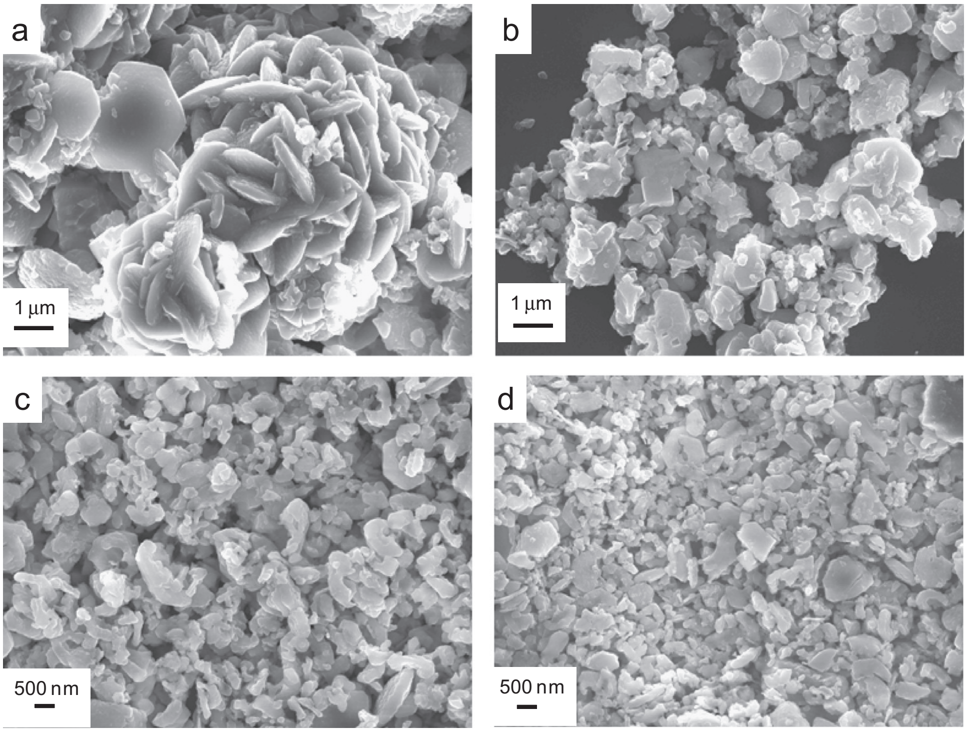

Fig. 7. FESEM microstructures of NaA zeolite powders obtained at 100 °C for (a) 15h, (b) 24h, and those of NaP zeolite powders synthesized at 100 °C for (c) 72h and (d) 96h.

zeolite [18]. It is interesting to point out that with increase in reaction time, the more fragmented particles enhanced the entropy of the system leading to the formation of thermodynamically stable phase of NaP zeolite.

4. Conclusion

NaA and NaP zeolite powders were synthesized through in-situ extraction of silica from agro-waste material, rice husk ash in the presence of organic-free precursors by a cost effective process. With the same molar composition of the precursors, crystallization of NaA and NaP took place at 100 °C by changing the synthesis times. The BET surface area and pore volumes of the synthesized powders decreased with increase in reaction times. Morphology of the powders changed with increase in synthesis times. With increase in reaction time, metastable NaA zeolite was transformed to more thermodynamically stable NaP zeolite. Locally available agro-waste material, RHA which is environmentally hazardous can be converted to advanced zeolite and zeolite-type materials by an economic and environmentally friendly process.

Acknowledgments

The authors would like to thank the Director of this Institute for his kind permission to publish this paper. They also acknowledge the help rendered by Material Characterization Division for Material Characterizations. One of the authors (S. Bohra) is thankful to Manipal Institute of Technology, Karnataka for giving her permission to carry out her M. Tech Thesis work in CSIR-CGCRI. The work was funded by the Institute's Project of CSIR-CGCRI, under Project no. OLP 299.

References

[1] D.W. Breck, Zeolite Molecular Sieves, John Wiley & Sons, London, 1974.
[2] R.M. Barrer, The Hydrothermal Chemistry of Zeolites, Academic Press, London, 1982.
[3] Y. Huang, D. Dong, J. Yao, L. He, J. Ho, C. Kong, A.J. Hill, H. Wang, In situ crystallization of macroporous monoliths with hollow NaP zeolite structure, Chemistry of Materials 22 (2010) 5271–5278.
[4] S. Chandrasekhar, K.G. Satyanarayana, P.N. Pramada, P. Raghavan, T. N. Gupta, Review processing, properties and applications of reactive silica from rice husk—an overview, Journal of Materials Science 38 (2003) 3159–3168.
[5] R.K. Vempati, US Patent 6444186 B1, 2002.
[6] M.K. Naskar, D. Kundu, M. Chatterjee, Coral-like hydroxy sodalite particles from rice husk ash as silica source, Materials Letters 65 (2011) 3408–3410.
[7] K.P. Dey, S. Ghosh, M.K. Naskar, A facile synthesis of ZSM-11 zeolite particles using rice husk ash as silica source, Materials Letters 87 (2012) 87–89.
[8] M.K. Naskar, D. Kundu, M. Chatterjee, A facile hydrothermal conversion of rice husk ash to ZSM-5 zeolite powders, Journal of the American Ceramic Society 95 (2012) 925–930.
[9] K.P. Dey, S. Ghosh, M.K. Naskar, Organic template-free synthesis of ZSM-5 zeolite particles using rice husk ash as silica source, Ceramics International 39 (2013) 2153–2157.
[10] Z. Ghasemi, H. Younesi, Preparation and characterization of nanozeolite NaA from rice husk at room temperature with organic additives, Journal of Nanomaterials (2011)http://dx.doi.org/10.1155/2011/858961.
[11] W.-C. Tan, S.-Y. Yap, A. Matsumoto, R. Othman, F.Y. Yeoh, Synthesis and characterization of zeolites NaA and NaY from rice husk ash, Adsorption 17 (2011) 863–868.
[12] S.N. Azizi, M. Yousefpour, Synthesis of zeolites NaA and analcime using rice husk ash as silica source without using organic template, Journal of Materials Science 45 (2010) 5692–5697.
[13] A.M. Yusof, N.A. Nizam, N.A.A. Rashid, Hydrothermal conversion of rice husk ash to faujasite-types and NaA-type of zeolites, Journal of Porous Materials 17 (2010) 39–47.
[14] R.V. Krishnarao, J. Subrahmanyam, T. Jagadish Kumar, Studies on the formation of black particles in rice husk silica ash, Journal of the European Ceramic Society 21 (2001) 99–104.
[15] H. Hamdan, M.N.M. Muhid, S. Endud, E. Listiorini, Z. Ramli, Si MAS NMR, XRD and FESEM studies of rice husk silica for the synthesis of zeolites, Journal of Non-Crystalline Solids 211 (1997) 126–131.
[16] K.P. Dey, D. Kundu, M. Chatterjee, M.K. Naskar, Preparation of NaA zeolite membranes using poly(ethyleneimine) as buffer layer, and study of their permeation behavior, Journal of the American Ceramic Society 96 (2013) 68–72.
[17] V.L. Zholobenko, J. Dwyer, R. Zhang, A.P. Chapple, N.P Rhodes, J. A. Stuart, Structural transition in zeolite P—an in situ FTIR study, Journal of the Chemical Society: Faraday Transactions 94 (1998) 1779–1781.
[18] R.M. Torres Sanchez, E.I. Basaldella, J.C. Tara, Zeolites surface reactions pointed out by charge parameters, Materials Letters 50 (2001) 138–144.